ISSN 1063-7788, Physics of Atomic Nuclei, 2021, Vol. 84, No. 6, pp. 1065–1069. © Pleiades Publishing, Ltd., 2021.

ELEMENTARY PARTICLES AND FIELDS
Experiment

Variations of Atmospheric Muons and Background Measured with Large Volume Detector

N. Yu. Agafonova[1)*], V. V. Ashikhmin[1)], E. A. Dobrynina[1)], R. I. Enikeev[1)], N. A. Filimonova[1),2)], O. G. Ryazhskaya[1)], I. R. Shakyrianova[1)], and V. F. Yakushev[1)]
(on behalf of the LVD Collaboration)

Received July 12, 2021; revised July 12, 2021; accepted July 12, 2021

Abstract—The analysis of atmospheric muons detected in the LVD underground experiment (Gran Sasso, Italy) has been completed. Atmospheric muons and the low-energy background that the LVD detects undergo annual (seasonal) variations. The background is created by gamma quanta from decays of ^{222}Rn daughter nuclei. Variations are due to seasonal fluctuations in radon concentration and additional injection of radon from groundwater associated with tectonic activity. At the LVD, research is underway to identify the relationship between the behavior of radon fields and seismic activity. The paper will discuss various sources of variations associated with geophysical aspects (the influence of the moon's motion; changes in pressure, humidity and temperature; seismic activity).

DOI: 10.1134/S1063778821130019

1. INTRODUCTION

The study of cosmic ray and background variations in underground experiments is important for low-background experiments to search for rare events. The dominant source of background in underground laboratories at low energies (0.5–5 MeV) is the spontaneous fission of uranium and thorium nuclei and their daughter nuclei (mainly radon). In the energy range (>5 MeV), the background source is neutrons from the αn-reaction from radon and neutrons from cosmic ray muons.

The connection between changes in the background in cosmic ray measurements and various geoeffects and technogenic factors is observed and discussed in many works [1–3]. A change in the concentration of radon in the air of an underground laboratory may indicate tectonic activity in the earth's crust [3–5]. Variations in radon concentration also depend on meteorological parameters such as soil moisture, precipitation, temperature, atmospheric pressure and relative humidity [6–8]. The concentration of radon is strongly influenced by seasonal and diurnal effects, which were observed in several publications [2, 9].

[1)]Institute for Nuclear Research, Russian Academy of Sciences, Moscow, Russia.
[2)]Faculty of Physics and Energy Problems, Department of Fundamental Interactions and Cosmology, Moscow Institute of Physics and Technology (National Research University), Dolgoprudny, Russia.
[*]E-mail: Agafonova@inr.ru

We show that by studying the background of the LVD experiment designed to monitor supernova explosions, namely to detect neutrinos from collapsing stellar cores, many effects can be observed associated with variations in cosmic ray muons and radon underground.

2. DETECTOR DESCRIPTION

The main scientific goal of the long-term LVD experiment is the search for neutrino radiation from stellar collapses [10]. The Large Volume Detector (LVD) located in the underground laboratory of Gran Sasso (Italy, near the city of L'Aquila) at a depth of $\langle H \rangle = 3650$ m w.e., consists of 840 scintillation 1.5 m^3 counters filled with a liquid scintillator (C_nH_{2n}). For different scientific tasks, the detector has two energy thresholds: the upper $E_{\mathrm{HET}} = 4$ MeV, and the lower $E_{\mathrm{LET}} = 0.5$ MeV [11]. The low-energy threshold data is used to study the background of the experiment and control the operation of the counters.

The LVD is capable of detecting all types of neutrinos by reactions of interaction with the nuclei of substances included in its structure—hydrogen, carbon, iron. The main reaction of antineutrino interaction is inverse beta decay (IBD reaction) $\bar{\nu}_e + p \to e^+ + n$, which creates two detectable signals: the first signal is caused by a positron, and the next signal comes from the capture of a neutron by a proton ($E_\gamma =$ 2.2 MeV, average capture time of about 185 μs) or iron, which is part of the setup structure ($\langle E_\gamma \rangle \sim$ 7 MeV, $\tau \sim 110\ \mu$s).

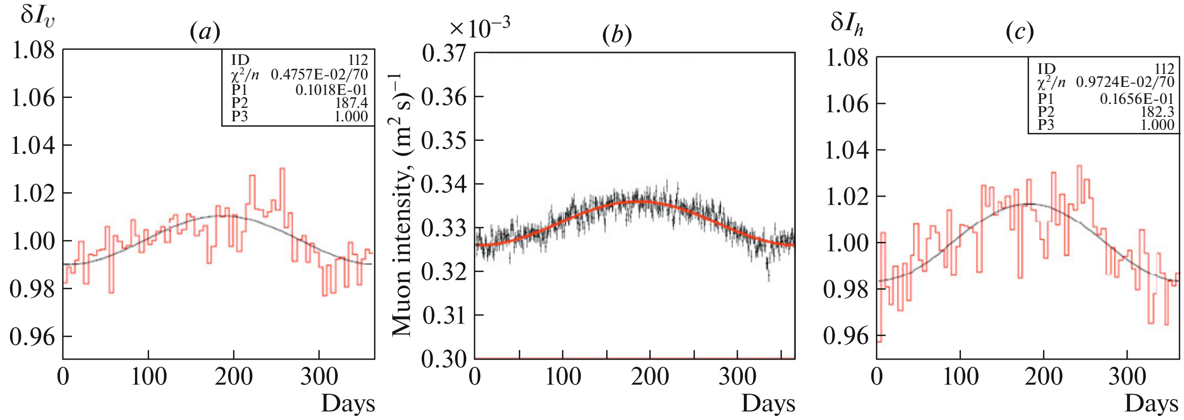

Fig. 1. Variations in the count rate of vertical muons (a), all muons (b), and horizontal muons (c), epoch superposition method. Bin for (a) and (c) is 5 days, for (b) is 1 day. Curves are approximation $f(t) = P3 + P1\cos(2\pi(t - P2)/365)$.

To detect atmospheric muons in the LVD setup, scintillation counters with an energy release of more than 50 MeV are used, which worked in a time range of less than 300 ns [12]. The average intensity of the registered muons is $I_\mu = 3.35 \times 10^{-4}\ \mathrm{m}^{-2}\ \mathrm{s}^{-1}$ [13]. The modular structure of the detector makes it possible to separate muons of the vertical and horizontal directions using the arrangement of the [14] counters.

3. VARIATION OF ATMOSPHERIC MUONS

The flux of atmospheric muons underground undergoes seasonal (annual) variations associated with changes in atmospheric temperature and the passage of muons through a thick layer of rock [15]. The positive temperature effect is associated with seasonal variations in the number of decays, mainly of the first generation of pions, which increases with the expansion of the atmosphere and decrease in the density of its upper layers (at an altitude of $\sim$30 km) in summer and vice versa—in winter.

Characteristics of seasonal variations in muon fluxes of different directions in the period from 2001 to 2018 were obtained from LVD data. The amplitude and phase of seasonal variations (Fig. 1) for horizontal and vertical muons were determined by the method of “independent simple hodoscopes.” The modulation amplitude for horizontal muons is $\delta I_h = (1.7 \pm 0.3)\%$. The modulation amplitude for vertical muons is $\delta I_v = (1.0 \pm 0.2)\%$ [14]. The variation amplitude of $\delta I_{\mathrm{tot}} = (1.56 \pm 0.08)\%$ for the total number of muons (all directions) detected by the setup was obtained [13].

4. LOW-ENERGY BACKGROUND VARIATION

Seasonal (annual) changes also experience a low-energy background, which is detected by the LVD (Fig. 2). This background is created by gamma quanta from decays of daughter nuclei of radon ^{222}Rn. Gamma radiation is generated mainly by bismuth nuclei, which, due to β-decay, transform into polonium with a characteristic time of 19.7 min. The energy spectrum of gamma radiation covers the range from 0.6 to 2.5 MeV. Based on experimental data from 2008 to 2016, using the epoch superposition method, the amplitude $(4 \pm 2)\%$ and phase (8.1 ± 0.4) month of seasonal variations in the background associated with the release of radon from the soil were obtained. Since radon is mainly carried by groundwater, its maximum concentration in the atmosphere of the hall is reached during the period of maximum water flow in the surrounding soil, that is, in September.

The detector also observes daily and weekly background variations [16]. As a result of the analysis of the data of the LVD on the low-energy threshold E_{LET}, the dependence of the radon concentration on the daily production activity in the underground halls of the Laboratory was established [17]. Weekly variations are associated with working and non-working days, and daily variations are associated with opening doors at the beginning and at the end of the working day.

The average concentration of radon ^{222}Rn in hall A, where the LVD detector is located, is $25 \pm 8\ \mathrm{Bq/m}^3$. We have observed a fairly noticeable correlation between background signals in the LVD and alpha decays due to ^{222}Rn [18].

A long-term analysis of the low-energy pulse $(C(r)/\langle C(r)\rangle)$ was carried out from 2001 to 2021. Figure 2 shows the time series of observations normalized to the average for 2019.

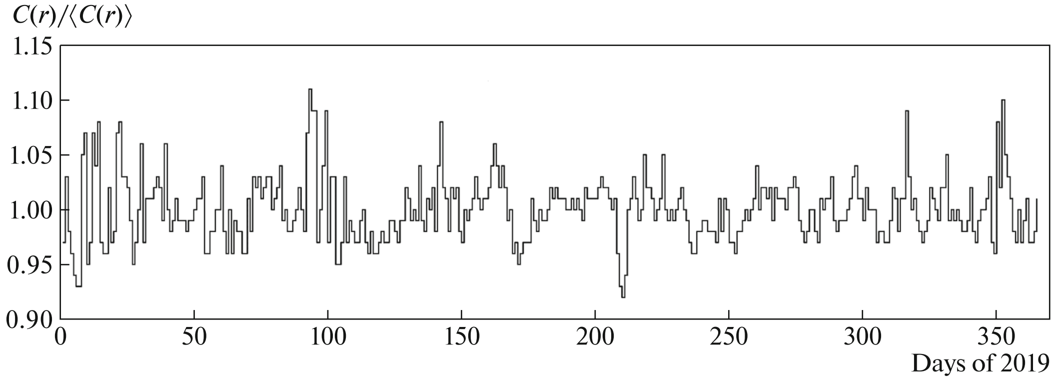

Fig. 2. Variations in low-energy background according to LVD data for 2019. There is 1 day in the bin.

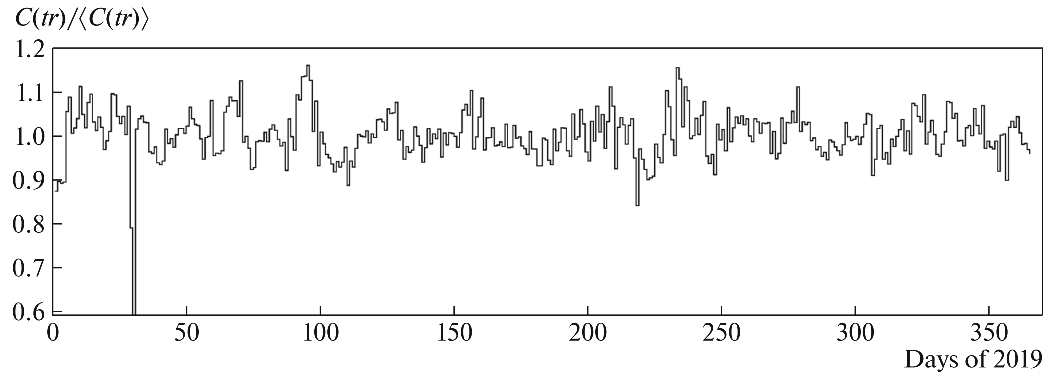

Fig. 3. Variations in high-energy background according to LVD data for 2019. There is 1 day in the bin.

5. HIGH-ENERGY BACKGROUND VARIATION

Another source of background in the energy range (above 5 MeV) are neutrons from the αn-reaction from radon decay and isolated neutrons from cosmic ray muons. These muons pass through the rock and do not enter the detector. Isolated are neutrons, the appearance of which is not associated with muons either in time or space. The spectrum of isolated neutrons underground is formed at the boundary between the rock and the experimental hall. Being equally likely generated over the volume of the rock, these neutrons pass through its various thicknesses and reach the walls of the hall. The total neutron flux from muons in the rock of the Gran Sasso laboratory is 4.58×10^{-10} cm^{-2} s^{-1} [19].

To find changes in the counting rate of high-energy (trigger pulses with $E_{\mathrm{HET}} > 5$ MeV) background events, we excluded muons and muon groups. We selected events in which only one triggering pulse was activated inside the detector (80 counters $\times$ 3 LVD towers). By this selection, we isolated pulses from gamma quanta from captures of neutrons on iron ($\langle E_\gamma \rangle \sim 7$ MeV) and pulses from recoil protons from the interaction of fast neutrons generated by muons that passed near the detector. In the analysis, we took into account only stable working counters, therefore the number of pulses is given per counter. Figure 3 shows the data of the high-energy background ($C(\mathrm{tr})/\langle C(\mathrm{tr})\rangle$), normalized to the average value for 2019.

6. EFFECT OF GEOPHYSICAL, TECHNOGENIC FACTORS AND SEISMIC ACTIVITY

The change in radon concentration is influenced by geophysical, technogenic factors and seismic activity, which leads to an accelerated release of radon from the rock (especially in sedimentary rocks).

Supply ventilation creates an excess of pressure, when the gate is opened, the pressure drops down and radon begins to come out of the walls intensively. Thus, opening and closing the gates to the room where the installation is located affects the counting rate of the detector. The passage of cars through the transport tunnel causes vibration of the ground, as a result of which the release of radon into the atmosphere of the hall increases. These sources of variation were studied on the LVD detector from low-energy background data in [20].

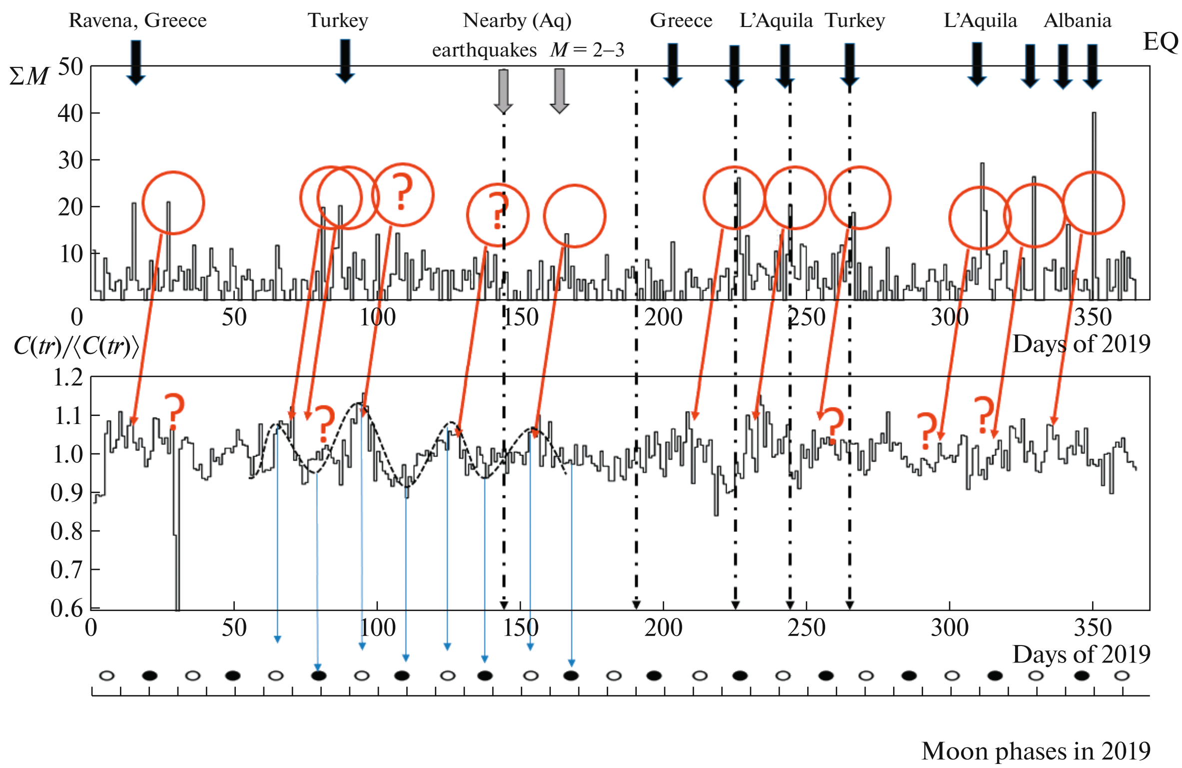

Fig. 4. The power of earthquake shocks per day (upper panel), and variations in the high-energy background ($C(tr)/\langle C(tr)\rangle$) according to LVD data (lower panel) for 2019. The arrows at the top show powerful earthquakes ($M > 4.5$) and their geographic location. Below are the phases of the full (•) and new moon (○).

The high water saturation of the Gran Sasso rock in summer leads to an accelerated transfer of radon; therefore, seasonal variations in the concentration of radon are observed [16].

The Apennine Peninsula is located at the junction of three tectonic plates: African, Eurasian and Adriatic (Apulian). Due to this complex geological structure, Italy is at risk. This region is characterized by mountain formations, volcanic and seismic activity. Seismic activity causes deformation of the earth's crust, as a result of which the number of microcracks increases, stress arises and vibration of the soil intensifies, which leads to a significant increase in the concentration of radon.

Using the data of the Italian National Institute of Geophysics and Volcanology [21], we plotted the dependence of the "power of earthquakes" per day for 2019. Within one day, we summed up the magnitudes ($M > 2$) at a distance of 250 km from the LVD setup (Fig. 4 (top panel)). This method was applied in the article [2]. It allows one to identify earthquakes with a sufficiently large "impact" on the earth's crust: if the earthquake was strong and was far away, but many small shocks near the detector, superimposed during the day, created a large "power." At the same time, small shocks at different times do not contribute and, most likely, do not affect the release of radon.

In Fig. 4 the thick arrows at the top show strong earthquakes. The strongest were November 7, 2019 near the LVD (L'Aquila) and November 26, 2019 in Albania (there were also a lot of aftershocks at the same time near the setup). We also noticed the fact that when strong aftershocks are observed in Turkey and Greece ($M > 5$), then at the same time there are many shocks of small magnitude ($M > 3.5$–4) in the area near the city of L'Aquila. This explains the ejection ($\Sigma M > 15$) in the top panel of Fig. 4.

Is it possible to compare the peaks in the "earthquake power" graph with peaks in the behavior of the background at the high-energy threshold? Assuming that an increase in stress in the earth's crust both at the moment and before an earthquake leads to an increased release of radon [22], one can try to see the peaks (10 days before the earthquake).

The tidal forces associated with the lunar cycle are likely to increase the release of radon. Figure 4 below shows the phases of the moon in 2019. Four periods can be distinguished where there is an increase in the high-energy background during the new moon and its decrease during the full moon (period from 60 to 170 days of the year). In Fig. 4, this period is marked with thin arrows and a dashed curve describing the data. However, this pattern disappears outside of this period. Dashed long arrows show the moments of severe thunderstorms in Italy in 2019.

7. CONCLUSIONS

The change in radon concentration is influenced by geophysical, technogenic factors and seismic activity, leading to an accelerated release of Rn from the soil (especially in the condition of sedimentary rocks).

Our measurements show that the background of the neutrino detector in different energy ranges is sensitive to different effects associated with the release of radon. It is necessary to further study the relationship of these effects with the involvement of seismic stations and instruments, such as, for example, the lidar [23] to study the precursors of earthquakes. Joint research of different technologies may provide a chance for the development of new algorithms for earthquake prediction.

REFERENCES

1. A. Bassignani, B. B. Bam, G. Colombo, H. Dekhissi, R. Fresca Fantoni, G. Giacomelli, G. Maltoni Giacomelli, and C. Sartorio, Radiat. Meas. **25**, 557 (1995).
2. V. V. Alekseenko, Yu. M. Gavrilyuk, D. M. Gromushkin, D. D. Dzhappuev, A. U. Kudzhaev, V. V. Kuzminov, O. I. Mikhailova, Yu. V. Stenkin, and V. I. Stepanov, Izv., Phys. Solid Earth **45**, 709 (2009).
3. Yu. Stenkin, V. Alekseenko, Z. Cai, Zh. Cao, C. Cattaneo, S. Cui, P. Firstov, E. Giroletti, X. Guo, H. He, Ye Liu, X. Ma, O. Shchegolev, P. Vallania, C. Vigorito, Y. Yanina, and J. Zhao, J. Environ. Radioact. **208–209**, 105981 (2019).
4. C. Y. King, J. Geophys. Res. **91**, 12269 (1986).
5. J. Planinic, V. Radolic, and B. Vukovic, Nucl. Instrum. Methods Phys. Res., Sect. A **530**, 568 (2004).
6. H. W. Kraner, G. L. Schroeder, and R. D. Evans, in *Proceedings of the Symposium on Natural Radiation and Environment, Houston, Texas, April 10–13, 1963,* Ed. by J. A. S. Adams and W. M. Lowder (Univ. Chicago Press, Chicago, 1964), p. 191.
7. M. Singh, R. C. Ramola, N. P. Singh, S. Singh, and H. S. Virk, J. Assoc. Explor. Geophys. **9**, 85 (1988).
8. V. Walia, H. S. Virk, T. F. Yang, S. Mahajan, M. Walia, and B. S. Bajwa, Terr. Atm. Ocean. Sci. **16**, 775 (2005).
9. S. Omori, S. Kita, S. Maruyama, and M. Santosh, Gondwana Res. **16**, 458 (2009).
10. N. Y. Agafonova, M. Aglietta, P. Antonioli, V. V. Ashikhmin, G. Badino, G. Bari, R. Bertoni, E. Bressan, G. Bruno, V. L. Dadykin, E. A. Dobrynina, R. I. Enikeev, W. Fulgione, P. Galeotti, M. Garbini, P. L. Ghia, et al., Astrophys. J. **802**, 47 (2015).
11. G. Bari, M. Basile, G. Bruni, G. Cara Romeo, A. Castelvetri, L. Cifarelli, A. Contin, C. Del Papa, P. Giusti, G. Iacobucci, G. Maccarrone. T. Massam, R. Nania, V. O'Shea, F. Palmonari, E. Perotto, et al., Nucl. Instrum. Methods Phys. Res., Sect. A **264**, 5 (1988).
12. N. Yu. Agafonova, Cand. Sci. (Phys. Math.) Dissertation (Inst. Nucl. Res. RAS, Moscow, 2015).
13. N. Yu. Agafonova, M. Aglietta, P. Antonioli, V. V. Ashikhmin, G. Bari, G. Bruno, E. A. Dobrynina, R. I. Enikeev, W. Fulgione, P. Galeotti, M. Garbini, P. L. Ghia, P. Giusti, E. Kemp, A. S. Malgin, A. Molinario, et al. (LVD Collab.), Phys. Rev. D **100**, 062002 (2019).
14. N. Y. Agafonova, V. V. Ashikhmin, E. A. Dobrynina, A. S. Malgin, O. G. Ryazhskaya, and I. R. Shakiryanova, Phys. At. Nucl. **83**, 69 (2020).
15. N. Yu. Agafonova and A. S. Malgin, J. Exp. Theor. Phys. **132**, 73 (2021).
16. N. Yu. Agafonova, V. V. Ashikhmin, E. A. Dobrynina, R. I. Enikeev, A. S. Malgin, K. R. Rudakov, O. G. Ryazhskaya, I. R. Shakiryanova, V. F. Yakushev, and the LVD Collab., Bull. Russ. Acad. Sci.: Phys. **83**, 614 (2019).
17. G. Bruno, J. Phys.: Conf. Ser. **203**, 012091 (2010).
18. G. Bruno and H. Menghetti, J. Phys.: Conf. Ser. **39**, 278 (2006).
19. A. S. Malgin, Phys. At. Nucl. **78**, 835 (2015).
20. N. Yu. Agafonova, V. A. Alekseev, E. A. Dobrynina, V. V. Kuznetsov, A. S. Mal'gin, O. G. Ryazhskaya, and V. F. Yakushev, INP Preprint No. 1071/2001 (Inst. Nucl. Res. RAS, Moscow, 2001).
21. National Institute of Geophysics and Volcanology of Italy. http://cnt.rm.ingv.it/.
22. H. S. Virk, Himalayan Geol. **17**, 91 (1996).
23. S. M. Pershin, V. A. Alekseev, N. G. Alekseeva, A. D. Zhigalin, V. S. Makarov, and A. V. Tiurin, Monitor. Sci. Technol. **3**, 6 (2010).